

Complementary collider and astrophysical probes of multi-component Dark Matter

J. Hernández-Sánchez^{*1}, V. Keus^{†2,3,4}, S. Moretti^{‡4,5,6}, D. Sokolowska^{§7,8}

¹ *Instituto de Física and Facultad de Ciencias de la Electrónica,
Benemérita Universidad Autónoma de Puebla, Apdo. Postal 542, C.P. 72570 Puebla, México,*

² *Dublin Institute for Advanced Studies, School of Theoretical Physics,
10 Burlington road, Dublin, D04 C932, Ireland*

³ *Department of Physics and Helsinki Institute of Physics,
Gustaf Hallstromin katu 2, FIN-00014 University of Helsinki, Finland*

⁴ *School of Physics and Astronomy, University of Southampton,
Southampton, SO17 1BJ, United Kingdom*

⁵ *Particle Physics Department, Rutherford Appleton Laboratory,
Chilton, Didcot, Oxon OX11 0QX, United Kingdom*

⁶ *Department of Physics and Astronomy, Uppsala University,
Box 516, SE-751 20 Uppsala, Sweden*

⁷ *University of Warsaw, Faculty of Physics, Pasteura 5, 02-093 Warsaw, Poland.*

⁸ *International Institute of Physics, Universidade Federal do Rio Grande do Norte,
Campus Universitario, Lagoa Nova, Natal-RN 59078-970, Brazil*

Abstract

We study a new physics scenario with two inert and one active scalar doublets, hence a 3-Higgs Doublet Model (3HDM). We impose a $Z_2 \times Z'_2$ symmetry onto such a 3HDM with one inert doublet odd under the Z_2 transformation and the other odd under the Z'_2 one. Such a construction leads to a two-component Dark Matter (DM) model. It has been shown that, when there is a sufficient mass difference between the two DM candidates, it is possible to probe the light DM candidate in the nuclear recoil energy in direct detection experiments and the heavy DM component in the photon flux in indirect detection experiments. With the DM masses at the electroweak scale, we show that, independently of astrophysical probes, this model feature can be tested at the Large Hadron Collider via scalar cascade decays in $2\ell + \cancel{E}_T$ final states. We study several observable distributions whose shapes hint at the presence of the two different DM candidates.

*E-mail: jaime.hernandez@correo.buap.mx

†E-mail: venus@stp.dias.ie

‡E-mail: stefano@soton.ac.uk, stefano.moretti@physics.uu.se

§E-mail: dsokolowska@iip.ufrn.br

1 Introduction

The Standard Model (SM) of particle physics has been extensively tested and is in great agreement with experiment with its last particle – the Higgs boson h – discovered in 2012 with a mass of ≈ 125 GeV by the ATLAS and CMS experiments at the CERN Large Hadron Collider (LHC) [1, 2]. Although the properties of the observed state are in agreement with those of the SM Higgs boson, it is entirely possible that it is one member of an extended scalar sector.

In fact, although in agreement with experiment, the SM is understood to be incomplete with one of its shortcomings being the lack of a viable Dark Matter (DM) candidate in its particle content. The standard cosmological Λ CDM Model [3] requires DM to be a particle stable on cosmological time scales, cold (i.e., non-relativistic at the onset of galaxy formation), non-baryonic, neutral and weakly interacting: such a state does not exist in the SM. Within Beyond the SM (BSM) frameworks, many such candidates exist, with the most well-studied being the Weakly Interacting Massive Particles (WIMPs) [4–6] with masses between a few GeV and a few TeV. WIMPs are usually stable due to the conservation of a discrete symmetry, such as scalar DM candidates in non-minimal Higgs frameworks which are stabilised by the conserved discrete symmetry of the scalar potential, see, e.g., [7–14].

One of the simplest BSM scenarios which provides a scalar DM candidate is the Inert Doublet Model (IDM) [9], which contains one inert doublet plus one active (Higgs) doublet, hence also known as I(1+1)HDM. In this model, which has been studied extensively in the literature (see, e.g., [10, 12, 13]), the additional $SU(2)_W$ scalar doublet has the same SM quantum numbers as the SM Higgs doublet. One of the possible vacuum alignments in this model is $(v, 0)$ wherein the active (or Higgs) doublet acquires a non-zero Vacuum Expectation Value (VEV) while the inert (or dark) doublet does not develop a VEV and therefore does not take part in electroweak symmetry breaking. The Lagrangian and the vacuum are symmetric under a Z_2 group under which only the inert doublet is odd. Due to the conservation of this symmetry, the inert doublet provides a stable DM candidate: the lightest neutral Z_2 -odd particle.

In the I(1+1)HDM, for masses of DM smaller than $m_h/2$, the dark sector communicates with the SM mainly through the Higgs boson exchange which is a characteristic of all Higgs-portal models [15–17]. Such a set-up leads to the DM-Higgs coupling, g_{DMh} , dictating the DM annihilation rate $\langle\sigma v\rangle$, the DM-nucleon scattering cross-section σ_{DM-N} and the Higgs invisible decays. Simultaneous fulfilment of current experimental constraints for these three types of processes is a challenging task, as shown, e.g., in [18–20]. For heavier DM particles, the direct annihilation into pairs of gauge bosons usually results in a relic density below the observed value, with the exception of very heavy DM particles. A possible solution to this problem is breaking the simple relation between the annihilation rate and direct detection cross-section by introducing coannihilation processes between DM and other dark particles which are close in mass. Coannihilation processes (through constructive and/or destructive interference) can decrease or increase the effective annihilation cross-section, which in turn change the DM relic density value. In the I(1+1)HDM, the DM candidate could potentially coannihilate with the neutral or charged Z_2 -odd particles. However, in a vast region of the parameter space, this coannihilation is too efficient, which leads to a total relic density below the observed value [21–42].

In models with an extended inert sector, more coannihilation processes are available and lead to a much richer phenomenology, see, e.g., models with extra inert singlets [43–45] or inert doublets [14] and, within the framework of 3-Higgs Doublet Models (3HDMs), the I(2+1)HDM of Refs. [46–54]. Proposed by Weinberg in 1976 [55], 3HDMs are very well motivated scenarios [56, 57] due to their implications for flavour physics, CP-violation, baryogenesis and inflation [58–65].

Here, we study an I(2+1)HDM framework symmetric under a $Z_2 \times Z'_2$ group with one inert doublet odd under Z_2 and even under Z'_2 , and the other inert doublet even under Z_2 and odd under Z'_2 . The lightest particle from each inert doublet is a viable DM candidate, yielding a two-component DM model. In a previous study [66], we showed that other dark particles from both doublets influence the thermal evolution and decoupling rate of DM particles and significantly impact the final relic abundance. (A similar analysis was performed in the context of a supersymmetric model in [67].) When there is a sufficient mass difference between the two DM candidates, which are both typically at the Electro-Weak (EW) scale, we showed that the light DM component can be probed by the nuclear recoil energy in direct detection experiments while the heavy DM component appears through its contribution to the photon flux in indirect detection experiments.

In this paper, quite independently of astrophysical probes, we study collider signatures of the I(2+1)HDM, namely, scalar cascade decays in $2\ell + \cancel{E}_T$ final states at the LHC. Specifically, we analyse several observable distributions whose shapes hint at the presence of the two different DM candidates. The remainder of the paper is organised as follows. In Section 2, we present the model, its scalar mass spectrum and discuss theoretical and experimental constraints on its parameter space. In Section 3, we discuss the experimental probes of the model and construct some Benchmark Points (BPs). In Section 4, we present our results, and in Section 5, we conclude.

2 Potential, mass spectrum and constraints

2.1 The scalar potential

The most general $Z_2 \times Z'_2$ symmetric 3HDM potential has the following form [57, 68]:

$$\begin{aligned}
V &= V_0 + V_{Z_2 \times Z'_2}, \\
V_0 &= -\mu_1^2(\phi_1^\dagger\phi_1) - \mu_2^2(\phi_2^\dagger\phi_2) - \mu_3^2(\phi_3^\dagger\phi_3) + \lambda_{11}(\phi_1^\dagger\phi_1)^2 + \lambda_{22}(\phi_2^\dagger\phi_2)^2 + \lambda_{33}(\phi_3^\dagger\phi_3)^2 \\
&\quad + \lambda_{12}(\phi_1^\dagger\phi_1)(\phi_2^\dagger\phi_2) + \lambda_{23}(\phi_2^\dagger\phi_2)(\phi_3^\dagger\phi_3) + \lambda_{31}(\phi_3^\dagger\phi_3)(\phi_1^\dagger\phi_1) \\
&\quad + \lambda'_{12}(\phi_1^\dagger\phi_2)(\phi_2^\dagger\phi_1) + \lambda'_{23}(\phi_2^\dagger\phi_3)(\phi_3^\dagger\phi_2) + \lambda'_{31}(\phi_3^\dagger\phi_1)(\phi_1^\dagger\phi_3), \\
V_{Z_2 \times Z'_2} &= \lambda_1(\phi_1^\dagger\phi_2)^2 + \lambda_2(\phi_2^\dagger\phi_3)^2 + \lambda_3(\phi_3^\dagger\phi_1)^2 + \text{h.c.},
\end{aligned} \tag{1}$$

where V_0 is invariant under any phase rotation while $V_{Z_2 \times Z'_2}$ ensures the symmetry under the $Z_2 \times Z'_2$ group generated by

$$g_{Z_2} = \text{diag}(-1, 1, 1), \quad g_{Z'_2} = \text{diag}(1, -1, 1). \tag{2}$$

Under this charge assignment, all SM fields, including the Higgs doublet ϕ_3 , are even under both Z_2 and Z'_2 . The additional doublets, ϕ_1 and ϕ_2 are odd under Z_2 and Z'_2 , respectively. In this paper, we assume that all parameters in the potential are real, therefore, we do not introduce any explicit CP-violation in the scalar sector. In particular, we do not consider the possible effects of dark CP-violation, a feature that was introduced for the first time in [49] and further studied in [50, 51, 54, 69], which could indeed arise in an extended dark sector. However, there is still the possibility of spontaneous breaking of the CP symmetry in the active sector for particular choices of parameters, as discussed in [66]. This choice of vacuum is not considered in this paper as it cannot lead to the appearance of two DM candidates in the model.

The Yukawa interactions are set to ‘‘Type-I’’ interactions, i.e., only the third doublet, ϕ_3 , will couple to fermions:

$$\mathcal{L}_Y = \Gamma_{mn}^u \bar{q}_{m,L} \tilde{\phi}_3 u_{n,R} + \Gamma_{mn}^d \bar{q}_{m,L} \phi_3 d_{n,R} + \Gamma_{mn}^e \bar{l}_{m,L} \phi_3 e_{n,R} + \Gamma_{mn}^\nu \bar{l}_{m,L} \tilde{\phi}_3 \nu_{n,R} + \text{h.c.} \quad (3)$$

Following the $Z_2 \times Z'_2$ charge assignment, this choice of Yukawa interaction is the only one which will not lead to breaking of the imposed discrete symmetries. This also ensures that there are no Flavour Changing Neutral Currents (FCNCs), since fields from the doublets which do not develop VEVs, ϕ_1 and ϕ_2 , will not couple to fermions.

2.2 Mass spectrum and physical parameters

The 2Inert vacuum state, i.e., the one with two automatically stable inert particles, has the alignment $(0, 0, v)$ in which the composition of the doublets are

$$\phi_1 = \begin{pmatrix} H_1^+ \\ \frac{H_1 + iA_1}{\sqrt{2}} \end{pmatrix}, \quad \phi_2 = \begin{pmatrix} H_2^+ \\ \frac{H_2 + iA_2}{\sqrt{2}} \end{pmatrix}, \quad \phi_3 = \begin{pmatrix} H_3^+ \\ \frac{v + h + iA_3^0}{\sqrt{2}} \end{pmatrix}, \quad (4)$$

with the extremum condition for this state reading as

$$v^2 = \frac{\mu_3^2}{\lambda_{33}}. \quad (5)$$

The third doublet, ϕ_3 , plays the role of the SM Higgs doublet, with the Higgs particle h having, by construction, tree-level interactions with gauge bosons and fermions identical to those of the SM Higgs boson. Its mass is fixed through the tadpole conditions to be

$$m_h^2 = 2\mu_3^2 = 2v^2 \lambda_{33} \quad (6)$$

and the A_3^0 and H_3^\pm states are the would-be Goldstone bosons.

The two inert doublets, ϕ_1 and ϕ_2 , provide two DM candidates. Each doublet consists of two neutral particles¹, H_i and A_i , and one charged particle H_i^\pm with $i = 1, 2$. For the two

¹As it is the case in multi-scalar models with unbroken Z_2 symmetries, the inert scalars H_i and A_i have opposite CP parity, as evident from their gauge interactions, however, it is not possible to establish their definite CP properties, as they do not couple to fermions.

generations of inert scalars the mass spectrum is as follows:

$$m_{H_1}^2 = -\mu_1^2 + \frac{1}{2}(\lambda_{31} + \lambda'_{31} + 2\lambda_3)v^2 \equiv -\mu_1^2 + \Lambda_3 v^2, \quad (7)$$

$$m_{A_1}^2 = -\mu_1^2 + \frac{1}{2}(\lambda_{31} + \lambda'_{31} - 2\lambda_3)v^2 \equiv -\mu_1^2 + \bar{\Lambda}_3 v^2, \quad (8)$$

$$m_{H_1^\pm}^2 = -\mu_1^2 + \frac{1}{2}\lambda_{31}v^2 \quad (9)$$

and

$$m_{H_2}^2 = -\mu_2^2 + \frac{1}{2}(\lambda_{23} + \lambda'_{23} + 2\lambda_2)v^2 \equiv -\mu_2^2 + \Lambda_2 v^2, \quad (10)$$

$$m_{A_2}^2 = -\mu_2^2 + \frac{1}{2}(\lambda_{23} + \lambda'_{23} - 2\lambda_2)v^2 \equiv -\mu_2^2 + \bar{\Lambda}_2 v^2, \quad (11)$$

$$m_{H_2^\pm}^2 = -\mu_2^2 + \frac{1}{2}\lambda_{23}v^2. \quad (12)$$

Parameters of the potential can be rephrased in terms of physical observables, such as masses and couplings. The tree-level SM couplings in the gauge and fermionic sectors follow exactly the SM definitions. The relevant parameters arising from the extended scalar sector are: (i) masses of inert particles and the Higgs-DM couplings, which represent parameters from the visible sector; (ii) self-interaction parameters, which describe interaction within the dark sector. The full list is:

$$v^2, m_h^2, m_{H_1}^2, m_{H_2}^2, m_{A_1}^2, m_{A_2}^2, m_{H_1^\pm}^2, m_{H_2^\pm}^2, \Lambda_2, \Lambda_3, \Lambda_1, \lambda_{11}, \lambda_{22}, \lambda'_{12}, \lambda_{12}. \quad (13)$$

The self-couplings $\lambda_{11}, \lambda_{22}, \lambda'_{12}, \lambda_{12}$ correspond exactly to the terms in Eq. (1), while the relations between remaining parameters and our chosen physical basis are as follows:

$$\mu_1^2 = -m_{H_1}^2 + \Lambda_3 v^2, \quad (14)$$

$$\lambda_3 = (m_{H_1}^2 - m_{A_1}^2)/(2v^2), \quad (15)$$

$$\lambda'_{31} = (m_{H_1}^2 + m_{A_1}^2 - 2m_{H_1^\pm}^2)/v^2, \quad (16)$$

$$\lambda_{31} = 2\Lambda_3 - 2\lambda_3 - \lambda'_{31}, \quad (17)$$

$$\mu_2^2 = -m_{H_2}^2 + \Lambda_2 v^2, \quad (18)$$

$$\lambda_2 = (m_{H_2}^2 - m_{A_2}^2)/(2v^2), \quad (19)$$

$$\lambda'_{23} = (m_{H_2}^2 + m_{A_2}^2 - 2m_{H_2^\pm}^2)/v^2, \quad (20)$$

$$\lambda_{23} = 2\Lambda_2 - 2\lambda_2 - \lambda'_{23}, \quad (21)$$

$$\lambda_1 = 2\Lambda_1 - (\lambda_{12} + \lambda'_{12}). \quad (22)$$

In principle, any particle among (H_i, A_i, H_i^\pm) can be the lightest. Here, we dismiss the possibility of H_i^\pm being the lightest, as it would mean that DM candidate is a charged particle. Choosing between H_1 and A_1 (or H_2 and A_2) is related only to a change of the sign of the

quartic parameter λ_3 (λ_2) and has no impact on the ensuing phenomenology. Therefore, we will choose $m_{H_i} < m_{A_i}, m_{H_i^\pm}$, which leads to the following relations between the parameters:

$$\lambda_2 < 0, \quad \lambda_3 < 0, \quad \lambda'_{31} + 2\lambda_3 < 0, \quad \lambda'_{23} + 2\lambda_2 < 0. \quad (23)$$

Notice that, unlike many Z_N symmetric models, the two lightest states from two doublets are automatically stable, regardless of their mass hierarchy, as they are stabilised by different Z_2 symmetries.

2.3 Theoretical and experimental constraints

The parameters of the potential V are subject to a number of theoretical and experimental constraints (described in detail in [66]). Below, we summarise the constraints imposed on the model to ensure that all proposed BPs are in agreement with current theoretical and experimental knowledge.

Stability of the potential For the potential to be bounded from below (i.e., having a stable vacuum) the following conditions are required [70]:

$$\lambda_{ii} > 0, \quad i = 1, 2, 3, \quad (24)$$

$$\lambda_x > -2\sqrt{\lambda_{11}\lambda_{22}}, \quad \lambda_y > -2\sqrt{\lambda_{11}\lambda_{33}}, \quad \lambda_z > -2\sqrt{\lambda_{22}\lambda_{33}}, \quad (25)$$

$$\begin{cases} \sqrt{\lambda_{33}}\lambda_x + \sqrt{\lambda_{11}}\lambda_z + \sqrt{\lambda_{22}}\lambda_y \geq 0 \\ \text{or} \\ \lambda_{33}\lambda_x^2 + \lambda_{11}\lambda_z^2 + \lambda_{22}\lambda_y^2 - \lambda_{11}\lambda_{22}\lambda_{33} - 2\lambda_x\lambda_y\lambda_z < 0, \end{cases} \quad (26)$$

where

$$\lambda_x = \lambda_{12} + \min(0, \lambda'_{12} - 2|\lambda_1|), \quad (27)$$

$$\lambda_y = \lambda_{31} + \min(0, \lambda'_{31} - 2|\lambda_3|), \quad (28)$$

$$\lambda_z = \lambda_{23} + \min(0, \lambda'_{23} - 2|\lambda_2|). \quad (29)$$

As noted in [71], these conditions are in fact sufficient but not necessary, as it is possible to construct examples of this model in which the potential is bounded from below, but which violate conditions (24)–(26). We do not explore such a region of parameter space in this work.

Global minimum condition For $(0, 0, v)$ to be a local minimum, all mass-squared values have to be positive, and, for it to be a global minimum, i.e., the true vacuum, its energy, $\mathcal{V}_{2\text{Inert}}$, has to be lower than the energy of any other possible minima, \mathcal{V}_X , that exist at the same time (see discussion in [66]). Following the chosen mass order and resulting relations in Eq. (23) we arrive at the following conditions:

$$\text{Local minimum if:} \quad \begin{cases} v^2 = \mu_3^2/\lambda_{33} > 0 \\ \Lambda_2 > \mu_2^2/v^2 \\ \Lambda_3 > \mu_1^2/v^2. \end{cases} \quad (30)$$

$$\text{Global minimum if, in addition:} \quad \mathcal{V}_{2\text{Inert}} = -\frac{\mu_3^4}{4\lambda_{33}} < \mathcal{V}_X. \quad (31)$$

Perturbative unitarity We require that the scalar $2 \rightarrow 2$ scattering matrix is unitary, i.e., the absolute values of all eigenvalues of such a matrix for Goldstones, Higgs and dark states with specific hypercharge and isospin should be smaller than 8π . Furthermore, all quartic scalar couplings should be perturbative, i.e., $\lambda_i \leq 4\pi$.

EW Precision Observables (EWPOs) We demand a 2σ , i.e., 95% Confidence Level (CL) agreement with EWPOs which are parametrised through the EW oblique parameters S, T, U . Assuming an SM Higgs boson mass of $m_h = 125$ GeV, the central values of the oblique parameters are given by [72]:

$$\hat{S} = 0.05 \pm 0.11, \quad \hat{T} = 0.09 \pm 0.13, \quad \hat{U} = 0.01 \pm 0.11. \quad (32)$$

In the I(1+1)HDM these constraints impose a strict order on the masses of the inert particles, with two neutral dark scalars being lighter than the charged particle. Furthermore, mass splitting between heavier neutral scalar and charged scalar is limited to roughly 50 GeV. However, in the case of a $Z_2 \times Z'_2$ 3HDM, these conclusions are no longer necessary. Cancellations between contributions to S, T, U parameters from the two generations of dark particles may lead to a different mass orderings, where either of A_i or H_i^\pm is the heaviest, as well as to an increased mass splittings between these particles (for a detailed discussion, see [66]).

Collider searches for new physics The presence of additional scalars, especially if they are sufficiently light, can influence properties of SM particles, e.g., their decay channels and widths. We forbid decays of EW gauge bosons into new scalars by enforcing:

$$m_{H_i} + m_{H_i^\pm} \geq m_W^\pm, \quad m_{A_i} + m_{H_i^\pm} \geq m_W^\pm, \quad m_{H_i} + m_{A_i} \geq m_Z, \quad 2m_{H_i^\pm} \geq m_Z. \quad (33)$$

Furthermore, we adopt LEP 2 searches for supersymmetric particles re-interpreted for the I(1+1)HDM in order to exclude the region of masses where the following conditions are simultaneously satisfied [73] ($i = 1, 2$):

$$m_{A_i} \leq 100 \text{ GeV}, \quad m_{H_i} \leq 80 \text{ GeV}, \quad \Delta m = |m_{A_i} - m_{H_i}| \geq 8 \text{ GeV}, \quad (34)$$

since this would lead to a visible di-jet or di-lepton signal.

The model also must agree with null results for additional neutral scalar searches at the LHC. As discussed in [66], current searches at the LHC for multi-lepton final states with missing transverse energy, \cancel{E}_T , are, in general, not sensitive enough to probe the parameter space of this model. This is mainly due to a relatively large cut on \cancel{E}_T used in experimental analyses, which results in a reduced sensitivity to probe the viable parameter space of the I(2+1)HDM scenario. Notice also that, as new charged particles are inert and hence do not couple to fermions, they are not subject to many constraints present in the 2HDM framework, e.g., flavour bounds on the charged scalar mass from $b \rightarrow s\gamma$, are not applicable here.

Charged scalar mass and lifetime We take a model independent lower estimate on the masses of all charged states: $m_{H_i^\pm} > 70$ GeV ($i = 1, 2$) [74]. Furthermore, in this work we will not consider scenarios with possibly long-lived charged particles and, following [75], we set the limit for a charged state lifetime to be $\tau \leq 10^{-7}$ s.

Higgs mass and signal strengths The combined ATLAS and CMS result for the Higgs mass is [76]:

$$m_h = 125.09 \pm 0.21 \text{ (stat.)} \pm 0.11 \text{ (syst.) GeV.} \quad (35)$$

The Higgs particle detected at the LHC is in excellent agreement with the SM predictions. By construction, the h state in the **2Inert** vacuum in Eq. (4) is SM-like and its (tree-level) couplings to gluons, massive gauge bosons and fermions are identical to the SM values.

The Higgs total width can be modified through additional decays into light inert scalars, S , by contributing to the $h \rightarrow SS$ decay channel when $m_S \leq m_h/2$ as well as through modifications to decay channels already present in the SM, in particular, the $h \rightarrow \gamma\gamma$ decay. In this work we take the upper limit on the Higgs total decay width to be [77]:

$$\Gamma_{\text{tot}} \leq 9.1 \text{ MeV.} \quad (36)$$

The partial decay width $\Gamma(h \rightarrow \gamma\gamma)$ is modified with the respect to the SM through the presence of two charged inert scalars. In this work, we use the combined ATLAS and CMS limit for the signal strength [78]:

$$\mu_{\gamma\gamma} = 1.14^{+0.19}_{-0.018}, \quad (37)$$

ensuring a 2σ agreement with the observation.

The latest constraints on the Higgs invisible decays from CMS and ATLAS are [79, 80]:

$$\text{BR}(h \rightarrow \text{inv.}) < 0.19 \text{ (CMS), } 0.26 \text{ (ATLAS).} \quad (38)$$

These constraints significantly limit the allowed values of Higgs-inert couplings for light inert states.

DM constraints The total relic density is given by the sum of the contributions from both DM candidates H_1 and H_2 ,

$$\Omega_T h^2 = \Omega_{H_1} h^2 + \Omega_{H_2} h^2, \quad (39)$$

and is constrained by Planck data [81] to be:

$$\Omega_{\text{DM}} h^2 = 0.1200 \pm 0.0012. \quad (40)$$

The current strongest upper limit on the Spin-Independent (SI) scattering cross-section of DM particles off of nuclei, $\sigma_{\text{DM-N}}$, is provided by the XENON1T experiment and is relevant for all regions of DM mass [82]. Regarding indirect detection searches, for light DM particles annihilating into bb or $\tau\tau$, the strongest constraints come from the Fermi-LAT satellite, ruling out the canonical cross-section $\langle\sigma v\rangle \approx 3 \times 10^{-26} \text{ cm}^3/\text{s}$ for $m_{\text{DM}} \lesssim 100 \text{ GeV}$ [83]. For heavier DM candidates the PAMELA and Fermi-LAT experiments provide similar limits of $\langle\sigma v\rangle \approx 10^{-25} \text{ cm}^3/\text{s}$ for $m_{\text{DM}} = 200 \text{ GeV}$ in the $bb, \tau\tau$ or WW channels [84].

3 Experimental probes of the model

A detailed DM analysis of the $Z_2 \times Z'_2$ symmetric I(2+1)HDM was presented in [66], with an emphasis on astrophysical probes of it. Here we focus instead on the complementarity between astrophysical and collider tests of the model. In our present analysis, we use the `micrOMEGAs` package [85] to calculate the relic density of the two DM candidates. During the analysis we follow the standard assumptions included in the code, namely: 1) particles within the dark sector are in thermal equilibrium; 2) they have the same kinetic temperature as that of the SM particle bath; 3) the number densities of DM particles can differ from the equilibrium values once their number density multiplied by their annihilation cross-section becomes too small to compete with the expansion rate of the Universe.

The lightest particle in each family is a viable DM candidate. As discussed previously, without loss of generality, we can take H_1 from the first family and H_2 from the second family to be the respective DM candidates. However, other dark particles from both families have a significant impact on the final relic abundances of these two stable particles, as they influence the thermal evolution and decoupling rate of DM particles.

In the discussion that follows, x_a denotes any relevant dark particle for a particular process from a respective dark sector. There are two² distinct classes of processes that can influence number densities of dark particles in each sector. In the first class there are (co)annihilation processes of the type:

$$x_a x_a \rightarrow \text{SM SM}. \quad (41)$$

In this class of processes, we have the standard DM annihilation, $H_i H_i \rightarrow \text{SM SM}$ with $i = 1, 2$, whose product depends mostly on the mass of the DM particles: we observe mostly Higgs-mediated annihilation into fermions for relatively light DM ($m_{\text{DM}} \lesssim m_h/2$), while heavier DM particles annihilate predominantly into gauge boson pairs, either directly or through Higgs s -channel. In our calculations, we also include annihilation into virtual gauge bosons, as these processes have a significant impact on DM annihilation rates for medium DM masses ($m_h/2 \lesssim m_{\text{DM}} \lesssim m_{W^\pm}$). Furthermore, if the mass difference between the DM candidate and other neutral or charged inert scalars from the same generation is small, then coannihilation channels such as $H_i A_i \rightarrow Z \rightarrow \text{SM SM}$ play an essential role. This is, in fact, the dominant class of processes for relatively high DM masses ($m_{\text{DM}} \gtrsim 500 \text{ GeV}$), exactly as it happens in the I(1+1)HDM. We would like to stress that, due to the $Z_2 \times Z'_2$ imposed symmetry in this class of processes, the two DM sectors are separated. There are no vertices that involve fields from two separate families, e.g., Higgs or gauge bosons couple only to a pair of inert particles from the same generation.

The second class of processes is DM conversion in which a pair of heavier scalars from one generation converts, either directly or through interaction with an SM particle, into a pair of dark particles from the other generation:

$$x_a x_a \rightarrow x_b x_b. \quad (42)$$

²Due to the imposed symmetry there are no processes that would be classified as semi-annihilation, i.e., processes of the form $x_a x_b \rightarrow \text{SM } x_d$.

Note that the conversion between two generations of DM particles occurs even if all self-interaction couplings are switched off. In Fig. 1, diagrams (a) and (b) represent the same initial/final state where a pair of H_2 particles are converted to a pair of H_1 particles through either Higgs-mediated or direct conversion. Even if the self-interaction parameter Λ_1 was set to zero, there would still be a non-zero contribution coming from diagram (a), as long as both particles couple to the Higgs boson ($\Lambda_{2,3} \neq 0$). We expect cancellations or enhancements depending on the relative sign of $\Lambda_2\Lambda_3$ and Λ_1 . Furthermore, depending on the masses and couplings, we also need to take into account annihilation of heavier dark particles from the second generation directly into stable particles from the first generation, e.g., $A_2A_2 \rightarrow h \rightarrow H_1H_1$. All these processes are automatically included in our numerical analysis.

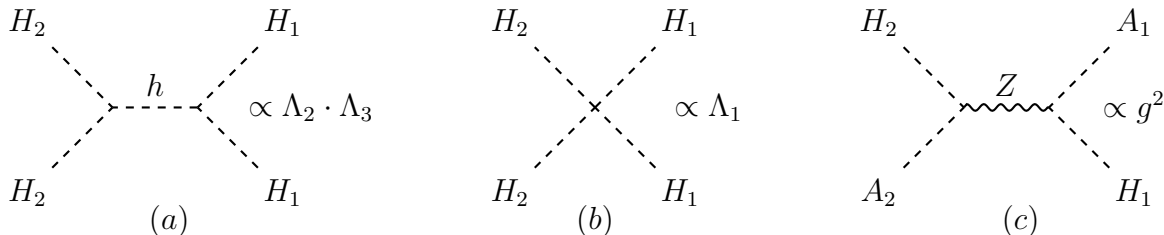


Figure 1: Example of DM conversion diagrams: (a) Higgs-mediated conversion of $H_2H_2 \rightarrow H_1H_1$, present always as long as $\Lambda_{2,3} \neq 0$; (b) direct DM conversion depending on the self-interaction parameter Λ_1 ; (c) Z -mediated conversion due to coannihilation channels.

As discussed in Section 2.2 in Eq. (13) we can parametrise the model by using masses of scalar particles and their couplings as follows.

1. The masses of the inert particles, $m_{H_1}^2, m_{H_2}^2, m_{A_1}^2, m_{A_2}^2, m_{H_1^\pm}^2, m_{H_2^\pm}^2$ dictate the annihilation patterns of DM particles. Depending on the absolute values of masses, but also on mass splittings between particles, we can expect different dominant channels of annihilation, coannihilation and conversion. Furthermore, both absolute and relative values of these masses will result in different possible collider signatures.
2. The couplings of the DM particles to the Higgs boson, Λ_2 and Λ_3 , govern not only DM annihilation and conversion but also influence possible invisible decays of the Higgs particle as well as direct and indirect detection of DM. In our numerical analysis we find that, in particular, the following vertices have significant impact on DM phenomenology:

$$g_{hH_1H_1} = 2\lambda_3 + \lambda_{31} + \lambda'_{31} = 2\Lambda_3, \quad (43)$$

$$g_{hH_2H_2} = 2\lambda_2 + \lambda_{23} + \lambda'_{23} = 2\Lambda_2, \quad (44)$$

$$g_{hA_1A_1} = -2\lambda_3 + \lambda_{31} + \lambda'_{31} = 2\Lambda_3 + 2(m_{A_1}^2 - m_{H_1}^2)/v^2, \quad (45)$$

$$g_{hA_2A_2} = -2\lambda_2 + \lambda_{23} + \lambda'_{23} = 2\Lambda_2 + 2(m_{A_2}^2 - m_{H_2}^2)/v^2. \quad (46)$$

3. The self-couplings of dark particles, $\lambda_1, \lambda'_{12}, \lambda_{12}$ and $\lambda_{11}, \lambda_{22}$, play two different roles. The first set governs interactions between two different families and will have an observable

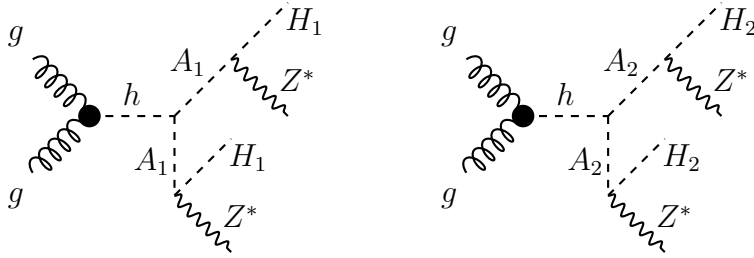


Figure 2: Diagrams leading to the $4\ell + \cancel{E}_T$ final state mediated by the h boson.

impact on DM relic abundance through DM conversion processes. In particular, the following couplings have a crucial impact on DM phenomenology:

$$g_{H_1H_1H_2H_2} = 2\lambda_1 + \lambda_{12} + \lambda'_{12} = 4\Lambda_1 - (\lambda_{12} + \lambda'_{12}), \quad (47)$$

$$g_{A_1A_1H_2H_2} = g_{A_2A_2H_1H_1} = -4\lambda_1 + \lambda_{12} + \lambda'_{12} = -4\Lambda_1 + 2(\lambda_{12} + \lambda'_{12}). \quad (48)$$

In turn, λ_{11} and λ_{22} do not directly contribute to any observable process and do not influence the DM abundance. They also have no impact on any observable collider processes. However, they have a fundamental impact on the range of other parameters through vacuum stability conditions.

Our numerical analysis shows that, due to the existence of the conversion processes, the total DM relic density receives its dominant contribution from H_1 while the contribution from H_2 is of a few percent of the total DM relic density.

3.1 BPs

In our previous analysis [66], we showed that, as a consequence of both DM candidate masses being in the EW region, astrophysical tools could be used to probe different DM components in a complementary way. The lighter DM candidate, H_1 , from which the total DM relic density receives dominant contribution, could have a detectable effect in the spectrum of the nuclear recoil energy measured at direct direction experiments (e.g., XENONnT/LZ or DARWIN) [86–88]. Complementary to that, the heavier DM candidate, H_2 , whose contribution to the total DM relic density is sub-dominant, may be detectable in its effect in enhancing the photon flux coming from the galactic centre measured at indirect detection experiments (e.g., FermiLAT) [89].

In the present paper, we focus on yet another complementary and independent probe of the two-component DM nature of this model, namely its collider signatures. We study scalar cascade decays into the two different DM candidates, H_1 and H_2 . Since the latter have comparable masses, we show that their presence is detectable simultaneously. Furthermore, their mass difference leads to different shapes in the distributions of several observables such as \cancel{E}_T and visible transverse momenta, as we will show.

Two candidates for relevant processes here would be $gg \rightarrow h \rightarrow A_1A_1 \rightarrow Z^*H_1Z^*H_1$ and $gg \rightarrow h \rightarrow A_2A_2 \rightarrow Z^*H_2Z^*H_2$, whose final states appear as $4\ell + \cancel{E}_T$, as shown in Fig. 2. Since

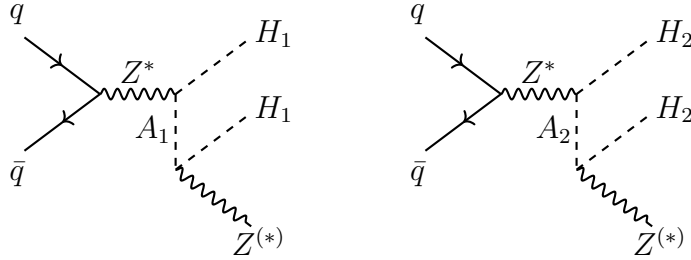


Figure 3: Diagrams leading to the $2\ell + \cancel{E}_T$ final state mediated by the Z boson.

the mass splitting of the two DM candidates, $m_{H_2} - m_{H_1}$, is larger than the \cancel{E}_T resolution at the LHC, one could potentially see the effect of the two DM components in different distributions. These channels are particularly interesting since they are sensitive to the hA_1A_1 and hA_2A_2 couplings, which highlight an important characteristic of the model, i.e., the fact that, due to the sub-dominant relic density of H_2 , the couplings of the heavier DM family to the SM-like Higgs boson could be exceptionally large ($g_{hA_2A_2} \sim 0.5$) while still in agreement with all collider and astrophysical bounds. However, the cross-sections for these processes are very small ($\sim 10^{-7}$ fb for the first family and $\sim 10^{-4}$ fb for the second family) to have any visible effect in collider searches. As a result, we do not discuss this process any further.

The ideal processes for our analysis are the $q\bar{q} \rightarrow Z^* \rightarrow H_1A_1 \rightarrow H_1H_1Z^*$ and $q\bar{q} \rightarrow Z^* \rightarrow H_2A_2 \rightarrow H_2H_2Z^*$ ones, whose final states appear as $2\ell + \cancel{E}_T$, as shown in Fig. 3. To highlight these signatures, we have chosen four BPs as shown in Tab. 1. The cross-sections for the $pp \rightarrow 2H_1 + 2\ell$ and $pp \rightarrow 2H_2 + 2\ell$ processes for the four BPs are shown in Tab. 2.

BP	m_{A_1}	$m_{H_1^\pm}$	m_{A_2}	$m_{H_2^\pm}$	Λ_2	$g_{hA_1A_1}$	$g_{hH_1^+H_1^-}$	$g_{hH_2H_2}$	$g_{hA_2A_2}$	$g_{hH_2^+H_2^-}$
L2n2	59.3	104.86	130.06	123.53	-0.0053	0.0336141	0.280793	-0.0106	0.217955	0.163227
L2p1	59.3	94.6	129.7	141	0.073	0.0336141	0.213159	0.146	0.371464	0.472558
L2p2	59.06	94.6	149.07	108.96	0.065	0.0326753	0.213159	0.13	0.533922	0.191877
L2p3	59.18	97.78	143.66	140.82	0.0099	0.0331442	0.233377	0.0198	0.371383	0.344682

Table 1: The four BPs, for which we have chosen $m_{H_1} = 50$ GeV, $m_{H_2} = 1000$ GeV and $g_{hH_1H_1} = 0.00002$, and we have set $\lambda_{11} = 0.11$, $\lambda_{22} = 0.12$, $\lambda_{12} = 0.121$, $\lambda'_{12} = 0.13$, $\Lambda_1 = \Lambda_3 = 0.00001$, the SM Higgs mass $m_h = 125$ GeV and the VEV $v = 246$ GeV, are in agreement with all astrophysical and collider constraints.

We now proceed to a Monte Carlo (MC) analysis of these BPs.

4 Numerical results

The integrated and differential cross-sections have been calculated using MadGraph [90] by adopting a generic LHC parameter card. Furthermore, we have used MadAnalysis [91] for constructing our selection, which involve basic cuts for leptons ℓ and jets j^3 : in pseudorapidity

³The latter being produced from QCD Initial State Radiation (ISR) and clustered with the Cambridge/Aachen algorithm with a 0.4 cone size [92, 93].

BP	$pp \rightarrow 2H_1 + 2\ell$	$pp \rightarrow 2H_2 + 2\ell$
L2n2	$\sigma = 1.058$ [fb]	$\sigma = 1.929$ [fb]
L2p1	$\sigma = 1.043$ [fb]	$\sigma = 1.912$ [fb]
L2p2	$\sigma = 0.9169$ [fb]	$\sigma = 1.230$ [fb]
L2p3	$\sigma = 0.9797$ [fb]	$\sigma = 2.448$ [fb]

Table 2: The cross-sections for the processes yielding $2\ell + \cancel{E}_T$ final states, whose leading contribution come from the $q\bar{q} \rightarrow Z^* \rightarrow H_1 A_1 \rightarrow H_1 H_1 Z^*$ and $q\bar{q} \rightarrow Z^* \rightarrow H_2 A_2 \rightarrow H_2 H_2 Z^*$ channels shown in Fig. 3.

$|\eta(\ell)|, |\eta(j)| < 3$, transverse momentum $p_T(\ell), p_T(j) > 10$ GeV as well as separation $\Delta R(j, \ell) > 0.5$. Finally, event rates have been computed considering 100 fb^{-1} of luminosity for the LHC machine.

The cross-sections for the two processes $q\bar{q} \rightarrow Z^* \rightarrow H_1 A_1 \rightarrow H_1 H_1 Z^*$ and $q\bar{q} \rightarrow Z^* \rightarrow H_2 A_2 \rightarrow H_2 H_2 Z^*$ given in Tab. 2 are instrumental to enable the extraction of distributions sensitive to the simultaneous presence of the two DM candidates at the forthcoming LHC Run 3 as they are both visible and comparable to each other. As mentioned before, in all four BPs presented herein, within each family the cross-section depends on both the absolute value of the masses involved and their mass splittings $M_{A_i} - M_{H_i}$ ($i = 1, 2$), with the latter having been chosen (in agreement with all astrophysical bounds) to be larger than or comparable to the expected experimental resolutions in (missing) transverse energy/momentum and (transverse or invariant) mass. Therefore, we shall be looking for differential spectra with a distinctive shape from which the existence of two different underpinning component distributions could be easily inferred. As a proof of concept, we show such observables for both the aforementioned two processes limitedly to one BP, e.g., L2n2. (Results are qualitatively similar for the other BPs, so we do not discuss these here.) For this choice, it is worth highlighting that the inert masses involved are as follows: $m_{H_1} = 50$ GeV with $m_{A_1} - m_{H_1} = 9.3$ GeV for one doublet and $m_{H_2} = 100$ GeV with $m_{A_2} - m_{H_2} = 30.06$ GeV for the other.

In Fig. 4, we show the \cancel{E}_T spectrum on the left and that of the transverse momentum of either lepton on the right, for the two channels $pp \rightarrow \ell\bar{\ell} + H_1 H_1$ and $pp \rightarrow \ell\bar{\ell} + H_2 H_2$ separately. The two sets of distributions are strikingly different so that, even when summed, one could clearly deduce the presence of two different DM candidates with different masses. In the \cancel{E}_T histogram, one can see two different peaks, a sharp one around 25 GeV for the H_1 case and a smoother one around 35 GeV for the H_2 case, this tracking the fact that $m_{H_1} \ll m_{H_2}$ (even though the presence of two DM particles in the event in each case spoils somewhat the correlations). In the p_T^ℓ spectra, it can be noticed the much sharper decrease of the H_1 distribution with respect to the H_2 one, this correlating to the fact that $m_{A_1} - m_{H_1} \ll m_{A_2} - m_{H_2}$.

In Fig. 5, one can notice that leptons are similarly central (see the pseudorapidity plot of either of these on the left) while their separation is noticeably different (see their cone size on the right) between the two DM candidates, the former spectrum showing that the overall events are not generally boosted but the Z^* itself can be so and differently between the H_1 and H_2 cases.

Fig. 6 shows the invariant mass of the leptons, defined through $M_{\ell\ell}^2 = (p_{\ell^+} + p_{\ell^-})^2$, which is

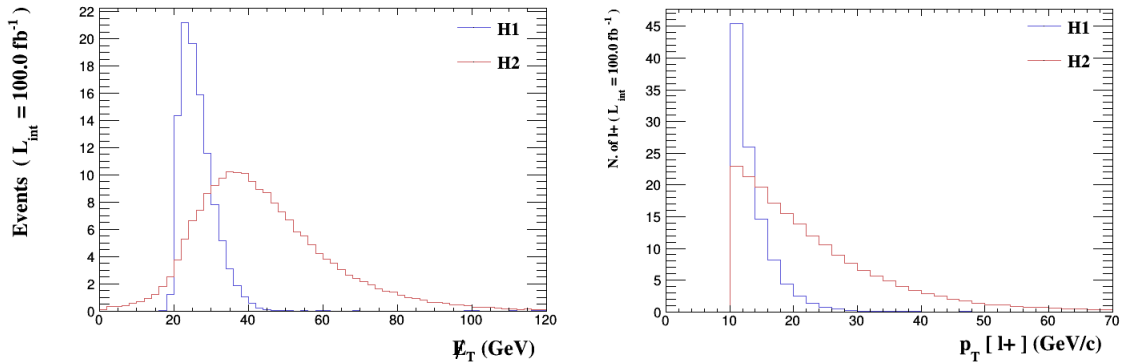


Figure 4: Missing transverse energy (left) and transverse momentum of either lepton (right) in the case of H_1 and H_2 separately.

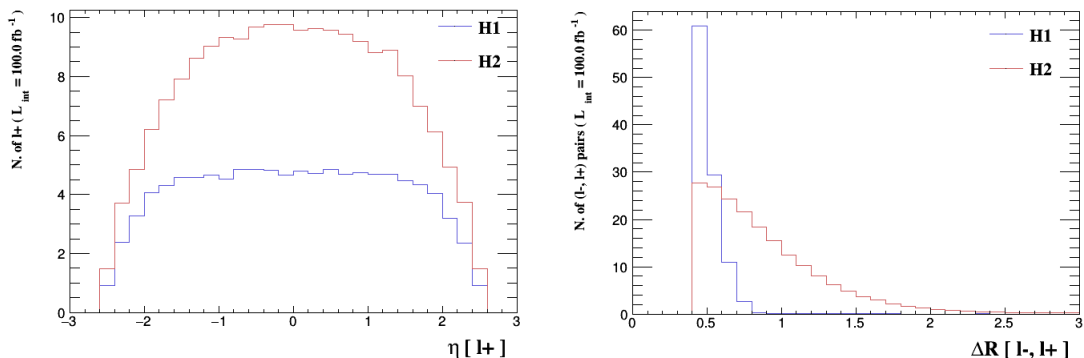


Figure 5: Pseudorapidity of either lepton (left) and separation between the leptons (right) in the case of H_1 and H_2 separately.

also correlated with the A_i and H_i mass splitting in each process, thus explaining the low mass peak for the H_1 case and the high mass peak for the H_2 case.

Fig. 7 shows the transverse mass of the final state leptons, defined through $M_T^2(\ell\ell) = (\sum_i E_{Ti})^2 - (\sum_i p_{Ti})^2$, which is rather strongly correlated to the A_1 and A_2 masses for the H_1 and H_2 cases, respectively.

Therefore, there exist several distributions which are significantly different in shape between the two DM candidates while also yielding sizeable event rates for LHC Run 3 luminosities, so that one could not only establish the presence of H_1 and H_2 simultaneously but also attempt to extract the underlying inert mass spectra from fitting the ensuing data to the I(2+1)HDM predictions. All this is clearly subject to validation through a MC analysis in presence of both reducible and irreducible backgrounds from the SM.

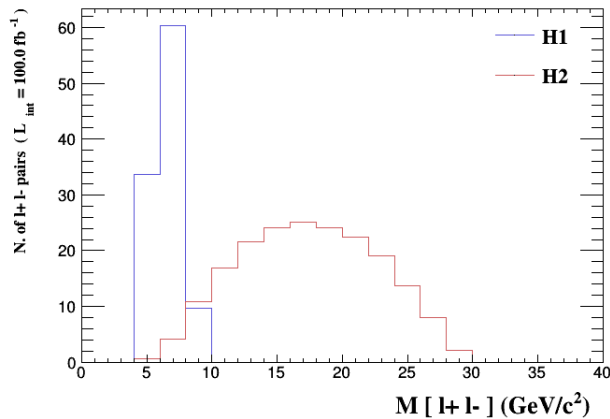


Figure 6: The invariant mass of the final state leptons in the case of H_1 and H_2 separately.

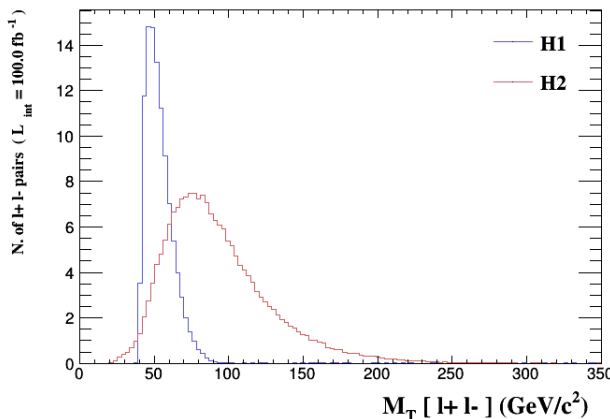


Figure 7: The transverse mass of the final state leptons and DM candidates in the case of H_1 and H_2 separately.

5 Conclusions

In this paper, we have studied a I(2+1)HDM framework symmetric under a $Z_2 \times Z'_2$ group with one inert doublet being odd under Z_2 and even under Z'_2 and the other inert doublet being even under Z_2 and odd under Z'_2 , while all SM particles transform trivially under the $Z_2 \times Z'_2$ symmetry. The lightest particle from each inert doublet is a viable DM candidate, resulting in a two-component DM model. In a recent publication [66], we showed that, when there is a sufficient mass difference between the two DM candidates, which are both typically at the EW scale, the light DM component can be probed by the nuclear recoil energy in direct detection experiments while the heavy DM component appears through its contribution to the photon flux in indirect detection experiments.

Here, in addition to such astrophysical probes, we have shown that certain collider signatures

can serve the same purpose; in each family, the decay of the heavier neutral inert state into the lighter one (i.e., the DM candidate) plus an off-shell (secondary) Z boson (decaying to di-lepton pairs) in association with an additional identical DM candidate emerging in parallel from primary production via an off-shell (primary) Z boson. The smoking-gun signature of this two-component DM scenario is thus $2\ell + \cancel{E}_T$, which can in fact be pursued already at the upcoming Run 3 of the LHC. Herein, one could study a variety of differential distributions stemming from this final state that would have a distinctive shape carrying the imprint of two underlying components, each corresponding to a different DM candidate. Indeed, those having an energy dimension could even be used to extract the underpinning inert state masses involved.

While these conclusions have been obtained without a signal-to-background analysis, we encourage ATLAS and CMS experimentalists to look into this novel phenomenology, as it would manifest itself in a well-studied final state at the LHC machine.

Acknowledgement

SM acknowledges support from the STFC Consolidated Grant ST/L000296/1 and is partially financed through the NExT Institute. DS is supported by the National Science Center, Poland, through the HARMONIA project under contract UMO-2015/18/M/ST2/00518. VK acknowledges financial support from the Academy of Finland projects “Particle cosmology and gravitational waves” No. 320123 and “Particle cosmology beyond the Standard Model” No. 310130. J H-S acknowledges support from SNI-CONACYT, PRODEP-SEP and VIEP-BUAP. The authors acknowledge the use of the IRIDIS High-Performance Computing Facility and associated support services at the University of Southampton in the completion of this work.

References

- [1] G. Aad *et al.* [ATLAS], Phys. Lett. B **716**, 1-29 (2012) [arXiv:1207.7214 [hep-ex]].
- [2] S. Chatrchyan *et al.* [CMS], Phys. Lett. B **716**, 30-61 (2012) [arXiv:1207.7235 [hep-ex]].
- [3] P. A. R. Ade *et al.* [Planck], Astron. Astrophys. **594**, A13 (2016) [arXiv:1502.01589 [astro-ph.CO]].
- [4] G. Jungman, M. Kamionkowski and K. Griest, Phys. Rept. **267**, 195-373 (1996) [arXiv:hep-ph/9506380 [hep-ph]].
- [5] G. Bertone, D. Hooper and J. Silk, Phys. Rept. **405**, 279-390 (2005) [arXiv:hep-ph/0404175 [hep-ph]].
- [6] L. Bergström, Rept. Prog. Phys. **63**, 793 (2000) [arXiv:hep-ph/0002126 [hep-ph]].
- [7] J. McDonald, Phys. Rev. D **50**, 3637-3649 (1994) [arXiv:hep-ph/0702143 [hep-ph]].

- [8] C. P. Burgess, M. Pospelov and T. ter Veldhuis, Nucl. Phys. B **619**, 709-728 (2001) [arXiv:hep-ph/0011335 [hep-ph]].
- [9] N. G. Deshpande and E. Ma, Phys. Rev. D **18**, 2574 (1978)
- [10] E. Ma, Phys. Rev. D **73**, 077301 (2006) [arXiv:hep-ph/0601225 [hep-ph]].
- [11] G. Belanger, K. Kannike, A. Pukhov and M. Raidal, JCAP **01**, 022 (2013) [arXiv:1211.1014 [hep-ph]].
- [12] R. Barbieri, L. J. Hall and V. S. Rychkov, Phys. Rev. D **74**, 015007 (2006) [arXiv:hep-ph/0603188 [hep-ph]].
- [13] L. Lopez Honorez, E. Nezri, J. F. Oliver and M. H. G. Tytgat, JCAP **02**, 028 (2007) [arXiv:hep-ph/0612275 [hep-ph]].
- [14] I. P. Ivanov and V. Keus, Phys. Rev. D **86**, 016004 (2012) [arXiv:1203.3426 [hep-ph]].
- [15] B. Patt and F. Wilczek, [arXiv:hep-ph/0605188 [hep-ph]].
- [16] X. Chu, T. Hambye and M. H. G. Tytgat, JCAP **05**, 034 (2012) [arXiv:1112.0493 [hep-ph]].
- [17] F. S. Queiroz and K. Sinha, Phys. Lett. B **735**, 69-74 (2014) [arXiv:1404.1400 [hep-ph]].
- [18] Y. Mambrini, Phys. Rev. D **84**, 115017 (2011) [arXiv:1108.0671 [hep-ph]].
- [19] A. Djouadi, O. Lebedev, Y. Mambrini and J. Quevillon, Phys. Lett. B **709**, 65-69 (2012) [arXiv:1112.3299 [hep-ph]].
- [20] A. Djouadi, A. Falkowski, Y. Mambrini and J. Quevillon, Eur. Phys. J. C **73**, no.6, 2455 (2013) [arXiv:1205.3169 [hep-ph]].
- [21] C. Arina, F. S. Ling and M. H. G. Tytgat, JCAP **10**, 018 (2009) [arXiv:0907.0430 [hep-ph]].
- [22] E. Nezri, M. H. G. Tytgat and G. Vertongen, JCAP **04**, 014 (2009) [arXiv:0901.2556 [hep-ph]].
- [23] X. Miao, S. Su and B. Thomas, Phys. Rev. D **82**, 035009 (2010) [arXiv:1005.0090 [hep-ph]].
- [24] M. Gustafsson, S. Rydbeck, L. Lopez-Honorez and E. Lundstrom, Phys. Rev. D **86**, 075019 (2012) [arXiv:1206.6316 [hep-ph]].
- [25] A. Arhrib, R. Benbrik and N. Gaur, Phys. Rev. D **85**, 095021 (2012) [arXiv:1201.2644 [hep-ph]].
- [26] M. Krawczyk, D. Sokołowska, P. Swaczyna and B. Świeżewska, Acta Phys. Polon. B **44**, no.11, 2163-2170 (2013) [arXiv:1309.7880 [hep-ph]].
- [27] A. Goudelis, B. Herrmann and O. Stål, JHEP **09**, 106 (2013) [arXiv:1303.3010 [hep-ph]].

- [28] A. Arhrib, Y. L. S. Tsai, Q. Yuan and T. C. Yuan, *JCAP* **06**, 030 (2014) [arXiv:1310.0358 [hep-ph]].
- [29] M. Krawczyk, M. Matej, D. Sokolowska and B. Świeżewska, *Acta Phys. Polon. B* **46**, no.1, 169-179 (2015) [arXiv:1501.04529 [hep-ph]].
- [30] A. Ilnicka, M. Krawczyk and T. Robens, *Phys. Rev. D* **93**, no.5, 055026 (2016) [arXiv:1508.01671 [hep-ph]].
- [31] M. A. Díaz, B. Koch and S. Urrutia-Quiroga, *Adv. High Energy Phys.* **2016**, 8278375 (2016) [arXiv:1511.04429 [hep-ph]].
- [32] K. P. Modak and D. Majumdar, *Astrophys. J. Suppl.* **219**, no.2, 37 (2015) [arXiv:1502.05682 [hep-ph]].
- [33] F. S. Queiroz and C. E. Yaguna, *JCAP* **02**, 038 (2016) [arXiv:1511.05967 [hep-ph]].
- [34] C. Garcia-Cely, M. Gustafsson and A. Ibarra, *JCAP* **02**, 043 (2016) [arXiv:1512.02801 [hep-ph]].
- [35] M. Hashemi and S. Najjari, *Eur. Phys. J. C* **77**, no.9, 592 (2017) [arXiv:1611.07827 [hep-ph]].
- [36] P. Poulose, S. Sahoo and K. Sridhar, *Phys. Lett. B* **765**, 300-306 (2017) [arXiv:1604.03045 [hep-ph]].
- [37] A. Alves, D. A. Camargo, A. G. Dias, R. Longas, C. C. Nishi and F. S. Queiroz, *JHEP* **10**, 015 (2016) [arXiv:1606.07086 [hep-ph]].
- [38] A. Datta, N. Ganguly, N. Khan and S. Rakshit, *Phys. Rev. D* **95**, no.1, 015017 (2017) [arXiv:1610.00648 [hep-ph]].
- [39] A. Belyaev, G. Cacciapaglia, I. P. Ivanov, F. Rojas-Abatte and M. Thomas, *Phys. Rev. D* **97**, no.3, 035011 (2018) [arXiv:1612.00511 [hep-ph]].
- [40] A. Belyaev, T. R. Fernandez Perez Tomei, P. G. Mercadante, C. S. Moon, S. Moretti, S. F. Novaes, L. Panizzi, F. Rojas and M. Thomas, *Phys. Rev. D* **99**, no.1, 015011 (2019) [arXiv:1809.00933 [hep-ph]].
- [41] D. Sokolowska, J. Kalinowski, J. Klamka, P. Sopicki, A. F. Zarnecki, W. Kotlarski and T. Robens, *PoS EPS-HEP2019*, 570 (2020) [arXiv:1911.06254 [hep-ph]].
- [42] J. Kalinowski, W. Kotlarski, T. Robens, D. Sokolowska and A. F. Zarnecki, *J. Phys. Conf. Ser.* **1586**, no.1, 012023 (2020) [arXiv:1903.04456 [hep-ph]].
- [43] G. Belanger, K. Kannike, A. Pukhov and M. Raidal, *JCAP* **04**, 010 (2012) [arXiv:1202.2962 [hep-ph]].

- [44] C. E. Yaguna and Ó. Zapata, JHEP **03**, 109 (2020) [arXiv:1911.05515 [hep-ph]].
- [45] G. Bélanger, A. Pukhov, C. E. Yaguna and Ó. Zapata, JHEP **09**, 030 (2020) [arXiv:2006.14922 [hep-ph]].
- [46] V. Keus, S. F. King, S. Moretti and D. Sokolowska, JHEP **11**, 016 (2014) [arXiv:1407.7859 [hep-ph]].
- [47] V. Keus, S. F. King and S. Moretti, Phys. Rev. D **90**, no.7, 075015 (2014) [arXiv:1408.0796 [hep-ph]].
- [48] V. Keus, S. F. King, S. Moretti and D. Sokolowska, JHEP **11**, 003 (2015) [arXiv:1507.08433 [hep-ph]].
- [49] A. Cordero-Cid, J. Hernández-Sánchez, V. Keus, S. F. King, S. Moretti, D. Rojas and D. Sokołowska, JHEP **12**, 014 (2016) [arXiv:1608.01673 [hep-ph]].
- [50] A. Cordero, J. Hernandez-Sanchez, V. Keus, S. F. King, S. Moretti, D. Rojas and D. Sokolowska, JHEP **05**, 030 (2018) [arXiv:1712.09598 [hep-ph]].
- [51] A. Cordero-Cid, J. Hernández-Sánchez, V. Keus, S. Moretti, D. Rojas and D. Sokołowska, Eur. Phys. J. C **80**, no.2, 135 (2020) [arXiv:1812.00820 [hep-ph]].
- [52] V. Keus, Phys. Rev. D **101**, no.7, 073007 (2020) [arXiv:1909.09234 [hep-ph]].
- [53] A. Aranda, D. Hernández-Otero, J. Hernández-Sanchez, V. Keus, S. Moretti, D. Rojas-Ciofalo and T. Shindou, Phys. Rev. D **103**, no.1, 015023 (2021) [arXiv:1907.12470 [hep-ph]].
- [54] A. Cordero-Cid, J. Hernández-Sánchez, V. Keus, S. Moretti, D. Rojas-Ciofalo and D. Sokołowska, Phys. Rev. D **101**, no.9, 095023 (2020) [arXiv:2002.04616 [hep-ph]].
- [55] S. Weinberg, Phys. Rev. Lett. **37**, 657 (1976)
- [56] I. P. Ivanov and E. Vdovin, Eur. Phys. J. C **73**, no.2, 2309 (2013) [arXiv:1210.6553 [hep-ph]].
- [57] V. Keus, S. F. King and S. Moretti, JHEP **01**, 052 (2014) [arXiv:1310.8253 [hep-ph]].
- [58] V. Keus and K. Tuominen, Phys. Rev. D **104**, no.6, 063533 (2021) [arXiv:2102.07777 [hep-ph]].
- [59] V. Keus, PoS **CORFU2019**, 059 (2020) [arXiv:2003.02141 [hep-ph]].
- [60] V. Keus, [arXiv:2105.05700 [hep-ph]].
- [61] H. Davoudiasl, I. M. Lewis and M. Sullivan, Phys. Rev. D **101**, no.5, 055010 (2020) [arXiv:1909.02044 [hep-ph]].

- [62] I. de Medeiros Varzielas, S. F. King, C. Luhn and T. Neder, Phys. Rev. D **94**, no.5, 056007 (2016) [arXiv:1603.06942 [hep-ph]].
- [63] F. Hartmann and W. Kilian, Eur. Phys. J. C **74**, 3055 (2014) [arXiv:1405.1901 [hep-ph]].
- [64] R. González Felipe, I. P. Ivanov, C. C. Nishi, H. Serôdio and J. P. Silva, Eur. Phys. J. C **74**, no.7, 2953 (2014) [arXiv:1401.5807 [hep-ph]].
- [65] F. R. Joaquim and J. T. Penedo, Phys. Rev. D **90**, no.3, 033011 (2014) [arXiv:1403.4925 [hep-ph]].
- [66] J. Hernandez-Sanchez, V. Keus, S. Moretti, D. Rojas-Ciofalo and D. Sokolowska, [arXiv:2012.11621 [hep-ph]].
- [67] S. Khalil, S. Moretti, D. Rojas-Ciofalo and H. Waltari, Phys. Rev. D **102**, no.7, 075039 (2020) [arXiv:2007.10966 [hep-ph]].
- [68] I. P. Ivanov, V. Keus and E. Vdovin, J. Phys. A **45**, 215201 (2012) [arXiv:1112.1660 [math-ph]].
- [69] V. Keus, PoS **CHARGED2016**, 017 (2016) [arXiv:1612.03629 [hep-ph]].
- [70] B. Grzadkowski, O. M. Ogreid and P. Osland, Phys. Rev. D **80**, 055013 (2009) [arXiv:0904.2173 [hep-ph]].
- [71] F. S. Faro and I. P. Ivanov, Phys. Rev. D **100**, no.3, 035038 (2019) [arXiv:1907.01963 [hep-ph]].
- [72] M. Baak *et al.* [Gfitter Group], Eur. Phys. J. C **74**, 3046 (2014) [arXiv:1407.3792 [hep-ph]].
- [73] E. Lundstrom, M. Gustafsson and J. Edsjo, Phys. Rev. D **79**, 035013 (2009) [arXiv:0810.3924 [hep-ph]].
- [74] A. Pierce and J. Thaler, JHEP **08**, 026 (2007) [arXiv:hep-ph/0703056 [hep-ph]].
- [75] J. Heisig, S. Kraml and A. Lessa, Phys. Lett. B **788**, 87-95 (2019) [arXiv:1808.05229 [hep-ph]].
- [76] G. Aad *et al.* [ATLAS and CMS], Phys. Rev. Lett. **114**, 191803 (2015) [arXiv:1503.07589 [hep-ex]].
- [77] A. M. Sirunyan *et al.* [CMS], Phys. Rev. D **99**, no.11, 112003 (2019) [arXiv:1901.00174 [hep-ex]].
- [78] G. Aad *et al.* [ATLAS and CMS], JHEP **08**, 045 (2016) [arXiv:1606.02266 [hep-ex]].
- [79] A. M. Sirunyan *et al.* [CMS], Phys. Lett. B **793**, 520-551 (2019) [arXiv:1809.05937 [hep-ex]].

- [80] M. Aaboud *et al.* [ATLAS], Phys. Rev. Lett. **122**, no.23, 231801 (2019) [arXiv:1904.05105 [hep-ex]].
- [81] N. Aghanim *et al.* [Planck], Astron. Astrophys. **641**, A6 (2020) [erratum: Astron. Astrophys. **652**, C4 (2021)] [arXiv:1807.06209 [astro-ph.CO]].
- [82] E. Aprile *et al.* [XENON], Phys. Rev. Lett. **121**, no.11, 111302 (2018) [arXiv:1805.12562 [astro-ph.CO]].
- [83] M. Ackermann *et al.* [Fermi-LAT], Phys. Rev. Lett. **115**, no.23, 231301 (2015) [arXiv:1503.02641 [astro-ph.HE]].
- [84] M. Cirelli and G. Giesen, JCAP **04**, 015 (2013) [arXiv:1301.7079 [hep-ph]].
- [85] G. Belanger, F. Boudjema, A. Pukhov and A. Semenov, Comput. Phys. Commun. **176**, 367-382 (2007) [arXiv:hep-ph/0607059 [hep-ph]].
- [86] E. Aprile *et al.* [XENON], JCAP **04**, 027 (2016) [arXiv:1512.07501 [physics.ins-det]].
- [87] J. Aalbers *et al.* [DARWIN], JCAP **11**, 017 (2016) [arXiv:1606.07001 [astro-ph.IM]].
- [88] L. Baudis, A. Ferella, A. Kish, A. Manalaysay, T. Marrodan Undagoitia and M. Schumann, JCAP **01**, 044 (2014) [arXiv:1309.7024 [physics.ins-det]].
- [89] M. Ackermann *et al.* [Fermi-LAT], Phys. Rev. D **86**, 022002 (2012) [arXiv:1205.2739 [astro-ph.HE]].
- [90] J. Alwall, R. Frederix, S. Frixione, V. Hirschi, F. Maltoni, O. Mattelaer, H. S. Shao, T. Stelzer, P. Torrielli and M. Zaro, JHEP **07**, 079 (2014) [arXiv:1405.0301 [hep-ph]].
- [91] E. Conte, B. Fuks and G. Serret, Comput. Phys. Commun. **184**, 222-256 (2013) [arXiv:1206.1599 [hep-ph]].
- [92] Y. L. Dokshitzer, G. D. Leder, S. Moretti and B. R. Webber, JHEP **08** (1997), 001 [arXiv:hep-ph/9707323 [hep-ph]].
- [93] M. Wobisch and T. Wengler, [arXiv:hep-ph/9907280 [hep-ph]].